ASSAY and Drug Development Technologies
Volume 5, Number 2, 2007

DOI: 10.1089/adt.2006.054

Validation of High Throughput Screening Assays Against Three Subtypes of Ca_V3 T-Type Channels Using Molecular and Pharmacologic Approaches

Xinmin Xie,[1] Amy L. Van Deusen,[2] Iuliia Vitko,[2] Daniella A. Babu,[3] Lucinda A. Davies,[2] Nhung Huynh,[1] Holden Cheng,[1] Naibo Yang,[4] Paula Q. Barrett,[2,3] and Edward Perez-Reyes[2,3]

Abstract: T-type Ca^{2+} channels encoded by voltage-gated Ca^{2+} channel (Ca_V) 3.1, 3.2, and 3.3 genes play important physiological roles and serve as therapeutic targets for neurological and cardiovascular disorders. Currently there is no selective T-channel blocker. To screen for such a blocker, we developed three stable cell lines expressing human recombinant $Ca_V3.1$, 3.2, or 3.3 channels and then examined their usefulness in high throughput screens. All three cell lines displayed an increase in intracellular Ca^{2+} in response to changes in extracellular Ca^{2+} as detected with Ca^{2+}-sensitive dyes using a fluorometric imaging plate reader (FLIPR® [Molecular Devices, Sunnyvale, CA] or FlexStation® [Molecular Devices]). The signal-to-noise ratio was 2–4. Co-expression of $Ca_V3.2$ with a mouse leak K^+ channel, which by virtue of being open at rest hyperpolarizes the cell membrane, blocked the fluorescent signal. Co-addition of KCl to these cells induced a Ca^{2+} signal that was similar to that observed in the cell line expressing $Ca_V3.2$ alone. These results confirm that the detection of intracellular Ca^{2+} increase in cells expressing $Ca_V3.2$ alone results from Ca^{2+} entry through channels that are open at the resting membrane potential of each cell line (*i.e.*, window currents). Testing known drugs on Ca_V3 channels showed that block could be reliably detected using the FlexStation assay, FLIPR assay, or voltage clamp recordings using the IonWorks® HT system (Molecular Devices). These results support the use of the FLIPR window current assay for primary drug screening and high throughput patch recordings for secondary screening of novel T-channel blockers.

Introduction

T-TYPE CA^{2+} CHANNELS are also called low voltage-activated channels because they open at voltages near the resting membrane potential of most cells. In many types of neurons, Ca^{2+} influx through T-type channels triggers low-threshold spikes, which in turn trigger a burst of action potentials mediated by Na^+ channels.[1] Burst firing is thought to play an important role in the synchronized activity of the thalamus observed in absence epilepsy, and also in a wider range of neurological disorders characterized by thalamocortical dysrhythmia.[2] Prominent T-currents are also observed in dorsal root ganglion neurons, with subsets of nociceptors expressing more T-current than high voltage-activated Ca^{2+} currents.[3] Considerable evidence supports the notion that a T-channel antagonist would be a useful drug for the treatment of pain and epilepsy.[4] Nevertheless, elucida-

[1]Bioscience Division, SRI International, Menlo Park, CA.
[2]Department of Pharmacology and [3]Molecular Medicine Graduate Program, University of Virginia, Charlottesville, VA.
[4]Molecular Devices Co., Sunnyvale, CA.

ABBREVIATIONS: $[Ca^{2+}]_i$, intracellular Ca^{2+} concentration; $[Ca^{2+}]_o$, extracellular Ca^{2+} concentration; Ca_v, voltage-gated Ca^{2+} channel; CV, coefficient of variation; DMSO, dimethyl sulfoxide; FLIPR, fluorometric imaging plate reader; Fluo-4-AM, Fluo-4 acetoxymethyl ester; HEK293, human embryonic kidney 293 cells; IC_{50}, concentration of half-maximal block (half of the maximum inhibitory response); TREK-1, TWIK-1-related K^+ channel.

tion of the physiologic and pharmacologic roles of T-type Ca^{2+} channels has been limited by the availability of selective and potent inhibitors. For example, the precise role T-channels play in the cardiovascular system remains controversial. Mibefradil, a potent T-channel blocker that also blocks L-type channels, is an effective antihypertensive agent; however, whether T-channel blockade contributed to its mechanism of action has been recently challenged.[5]

Molecular cloning revealed the existence of three T-type channel genes, designated voltage-gated Ca^{2+} channel (Ca_v) 3.1, 3.2, and 3.3 (also termed α1G, α1H, and α1I). Ca_v3.1 and Ca_v3.3 subtypes are expressed predominantly, though not exclusively, in the brain. In contrast, the Ca_v3.2 subtype is also present in the central nervous system, but appears to be relatively more abundant in several nonneuronal tissues, including heart, kidney, adrenal, and pituitary.[1] Deletion of the genes encoding Ca_v3 channels and studies of the resultant phenotypes have shed light on these aspects. Results from studies on Ca_v3.1 (α1G) Ca^{2+} channel knockout mice support the notion that T-currents are responsible for the generation of the slow wave spikes in the thalamus that are involved in epileptogenesis of absence seizures and sleep regulation.[6,7] In contrast, peripheral T-current inhibition with mibefradil produces analgesic effects.[8–10] The main target for these effects is Ca_v3.2, since disruption of its expression using either antisense oligonucleotides or transgenic mice produces analgesia.[11,12] It is hypothesized that subtype-selective Ca_v3 modulators should produce more specific pharmacological actions for a variety of neurological, psychiatric, and cardiovascular disorders, with fewer side effects. HTS of a large compound library is the initial step toward identifying such novel compounds.

The "gold standard" technology to study ion channels is with electrophysiologic techniques using whole-cell voltage-clamp recordings. However, the T-currents in native cells are usually very small (<100 pA).[1] In contrast, recombinant channels can be expressed at much higher levels (500–2,000 pA).[13] Notably, the electrophysiologic properties of recombinant Ca_v3 channels are similar to those of native T-type currents.[1] These cell lines offer a valuable tool for drug screening, yet screening by electrophysiologic techniques are laborious and time-consuming, and an HTS format for primary drug screening is difficult to achieve, even with the recently developed high throughput electrophysiology technology.[14,15] In this study we explore the possibility that T-channel activity can be assayed using a fluorometric method in HTS format. This assay exploits that ability of T-channels to open at the resting membrane potential of many cells, thereby producing a "window" current.[16] Chemin *et al*.[17] showed that recombinant T-channels also showed this activity when expressed in human embryonic kidney 293 (HEK293) cells; increasing extracellular Ca^{2+} concentration ($[Ca^{2+}]_o$) led to increases in intracellular Ca^{2+} concentration ($[Ca^{2+}]_i$). A similar increase in fluorescence was observed with recombinant Ca_v3.2 under the control of an inducible promoter.[18]

In the present study we used a background K^+ channel to confirm that these Ca-induced changes in fluorescence were attributable to T-channel window currents. We also show that all three Ca_v3 channels subtypes—Ca_v3.1, 3.2, and 3.3—are capable of generating this $[Ca^{2+}]_i$ signal. We describe conditions that optimize the detection and reproducibility of these signals on a fluorometric imaging plate reader (FLIPR®, Molecular Devices, Sunnyvale, CA). Finally, we show that these cell lines are suitable for use in an Ionworks® HT planar patch system, and compared the potency of a set of compounds determined by both fluorometric method and patch recording techniques.

Materials and Methods

Cell culture

Creation of HEK293 cell lines expressing human recombinant Ca_v3.1, 3.2, and 3.3 channels has been described previously.[13] All three cell lines were grown as monolayers in Dulbecco's Modified Eagle's Medium containing 4.5 g/L D-glucose, pyroxidine hydrochloride, and 0.5 m*M* $CaCl_2$, supplemented with 10% fetal bovine serum, 1 mg/ml geneticin, 4 m*M* L-glutamine, 100 U/ml penicillin, and 100 μg/ml streptomycin. A fourth cell line was created by transfecting HEK293 cells with two plasmids: one containing human Ca_v3.2 (conferring geneticin resistance), and the other containing a truncated mouse K^+ channel, the TWIK-1-related K^+ channel called TREK-1 (conferring puromycin resistance).[19] For measurement of $[Ca^{2+}]_i$ using the fluorometric methods, cells were seeded into clear-bottom (either clear or black-walled) 96-well microtiter plates that were coated with poly-D-lysine (Becton-Dickinson, Franklin Lakes, NJ) at a concentration range of 50,000–70,000 cells per well and used for assay within approximately 12 h.

Measurement of $[Ca^{2+}]_i$ using Ca-sensitive dyes

Ca_v3 cells were washed with 140 m*M* NaCl, 5 m*M* KCl, 10 m*M* glucose, 0.5 m*M* $CaCl_2$, and 10 m*M* HEPES at pH 7.4 (HBSS-HEPES buffer), using a multichannel pipettor (Multimek 96/384, Beckman Coulter, Fullerton, CA) prior to incubation with 2 μ*M* Fluo-4 acetoxymethyl ester (Fluo-4-AM) in HBSS-HEPES buffer for 30 min at 37°C. Cells were then washed again, overlaid with 100 μl of HBSS-HEPES buffer, and then loaded into a FlexStation® (Molecular Devices). For assays using Calcium 3 FLIPR dye, growth medium was removed by aspiration, 180 μl of Calcium 3 reagent reconstituted in HBSS-HEPES buffer was added, and cells were loaded for 60 min at 37°C. Test drugs were added to wells at desired

concentrations at room temperature and incubated for 20 min. Subsequently, the plates were placed on the FLIPR, and cells' fluorescence was monitored ($\lambda_{excitation}$ = 488 nm, $\lambda_{emission}$ = 540 nm) before and after the addition of HBSS-HEPES buffer containing a single or a range of $CaCl_2$ concentrations (0.5–20 m*M*). In the initial measurements, fluorescence intensity units were measured every 1 s for 60 s; for the next 2–6 min, measurements were taken every 10 s.

All compounds were dissolved in dimethyl sulfoxide (DMSO) as a stock solution and diluted to three or four times to the final concentrations with HBSS-HEPES buffer. Effects of DMSO on basal $[Ca^{2+}]_i$ assays were assessed. Concentrations below 0.3% have little effect, 0.3% decreased basal activity ~15%, while higher concentrations were clearly inhibitory. Therefore 0.3% DMSO was selected as the maximum.

Data analysis of FlexStation data

Fluorescence signals were acquired for 60 s and then analyzed using SoftMax Pro software (version 4.8, Molecular Devices). The initial 15 s of baseline were used to zero the signal, and the remaining signal was integrated using the area under the curve function. The results were exported to Excel (Microsoft, Bellevue, WA) spreadsheets. The results were normalized to the buffer control, averaged, and then fit with the following form of the Hill-Langmuir equation using the Solver function:

$$B = \frac{1}{(1 + (10^{\log((IC_{50} - [D]) \times h)})}$$

where B represents fractional block at the drug concentration D, h is the Hill coefficient, and IC_{50} is the concentration of half-maximal block (half of the maximum inhibitory response). Drug concentrations were converted to the base 10 logarithm. Figures were generated using Prism® software (GraphPad Software, San Diego, CA), and the smooth curves represent fits (same equation) to the average.

Data analysis of FLIPR data

A dilution/mechanical artifact always occurs on addition of the stimulus. Therefore, basal fluorescence was defined as that measured in the data point following the addition of the buffer stimulus. The peak value was measured by the maximum – minimum method. Data were represented as mean ± standard error of the mean of three to eight wells, and most experiments were repeated at least twice. High throughput assays can rapidly generate large datasets, and an automated or semiautomated process of data analysis is critical to HTS. The current proprietary FLIPR software can automatically quantitatively detect the signals and export them as text or Excel files. To facilitate analysis of these data, SRI (Menlo Park, CA) developed a user-friendly software using a combination of MATLAB® (version 6.5, The MathWorks, Natick, MA) and Excel. This program has the ability to automatically identify single concentration hits for HTS use and to perform standard concentration–response curve analysis for follow-up pharmacology. The program interfaces with a custom-made graphical user interface and built-in Tutorial for easy and self-taught learning.

Analyses of the FLIPR fluorescence response data were performed using algorithms programmed into MATLAB version 6.5 interfaced with a custom-made graphical user interface. The algorithm is designed to extract the maximum or minimum response peak with respect to the baseline of the sequence data. If multiple cells are selected, the algorithm calculates the average peak values, the standard deviations of the peak values, the standard error of the mean of the peak values, and the coefficient of variation (CV) of the peak values. Student's two-tail t test was used to calculate 95% confidence intervals. As an option, the user can also select wells that are defined as positive or negative controls.

Analyses of dose–response data were done using algorithms programmed in MATLAB version 6.5. The peak values and their respective confidence intervals were plotted as a function of the concentration values (in logarithmic base 10). The data were then fitted to a sigmoidal curve using least square fit (Eq. 1, adapted from SigmaPlot, Systat, San Jose, CA). The IC_{50} value was extracted from the best-fit curve using one of the following equations (see Fig. 4):

$$y = \frac{a + (b - a)}{1 + \frac{x}{c}} \quad (1)$$

In Eq. 1, a defines the amplitude, b is the y-intercept, c is the slope of the curve, and x is the compound concentration. A second equation was also used to fit the data (Eq. 2), using the same variables as Eq. 1:

$$y = \frac{a}{1 + \exp(cx - b)} \quad (2)$$

Both are logistic equations derived from the Hill-Langmuir equation. Equation 1 produces better fits (*i.e.*, smallest least square error) when in cases of incomplete block. Future development will expand the analyzed data to be stored in a database and associate them with the metadata describing the experiment (compounds, experimental conditions and protocol, etc.). The information should be combined with the raw and analyzed data and stored in a secure file system and database.

Assay quality control

A screening window coefficient, "*Z*-factor," which reflects both the assay signal dynamic range and the data

variation associated with the signal measurements,[20] was used to assess the assay quality. The *Z*-factor from the negative control (normal buffer containing 0.5 m*M* Ca) of three separate assays (plate-to-plate variability) was calculated as 0.5, indicating the consistency of the assay. For the positive control, a *Z*-factor of 0.5 was calculated from eight wells of maximal inhibition produced by a plateau concentration of mibefradil (30 μM) and control (10 m*M* Ca) in the same plate. However, in separate assays, the same experiment yielded a *Z*-factor of approximately 0.4, indicating that results of drug testing are more variable than those of the assay *per se*.

Patch clamp recording

Conventional patch clamp recording techniques were used for characterization of the three Ca_v3 channels expressed in HEK293 cell lines as described previously.[21] The IonWorks Quattro™ HT planar patch clamp system was used to test a number of known T-channel modulators with Ca_v3 channels. Cells were bathed with an extracellular solution containing 2 m*M* $CaCl_2$, 140 m*M* tetraethylammonium chloride, 6 m*M* CsCl, 0.1 m*M* EDTA, and 10 m*M* HEPES (pH adjusted to 7.4 with CsOH) at room temperature. The intracellular solution contained 55 m*M* CsCl, 75 m*M* $CsSO_4$, 10 m*M* $MgCl_2$, 0.1 m*M* EGTA, and 10 m*M* HEPES (pH adjusted to 7.2 with CsOH) plus 10 μg/ml amphotericin B. T-current amplitudes ranged from 50 to 500 pA when the extracellular solution contained 2 m*M* Ca^{2+} as charge carrier. Baseline current traces and after-compound application were recorded. Concentration-dependent inhibitory curves were constructed to estimate the IC_{50} of the test compounds.

Materials

Cell culture media and supplements were purchased from Gibco Invitrogen (Invitrogen, Carlsbad, CA). The following materials were obtained from the sources indicated: fetal bovine serum from Hyclone (Logan, UT), Calcium 3 FLIPR dye from Molecular Devices, and Fluo-4-AM from Molecular Probes (Eugene, OR). All other reagents and test drugs were purchased from Sigma-Aldrich (St. Louis, MO). The mibefradil used in the

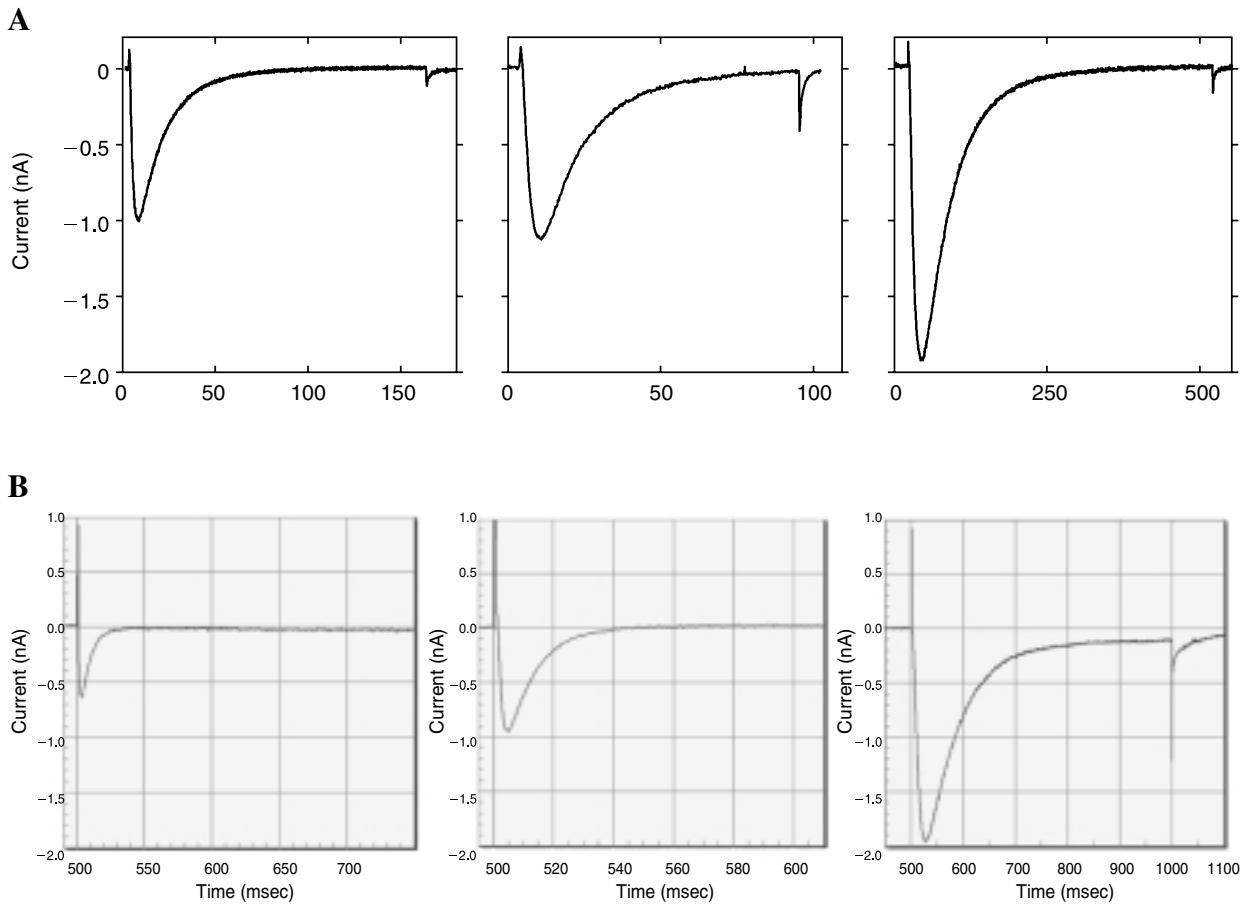

FIG. 1. Whole-cell Ca^{2+} currents recorded from three stable cell lines expressing $Ca_v3.1$, $Ca_v3.2$, or $Ca_v3.3$. The cells were held at −100 mV and then depolarized to −30 mV. (**A**) Representative traces obtained using traditional patch clamp recording with an Axon Instruments 200B amplifier (Molecular Devices): $Ca_v3.1$ (**left panel**), $Ca_v3.2$ (**middle panel**), and $Ca_v3.3$ (**right panel**). (**B**) Traces obtained using planar patch clamp recording with an IonWorks Quattro HT system.

FLIPR and IonWorks was obtained from Sigma-Aldrich, while mibefradil used in the FlexStation assay was a gift from Hoffmann-La Roche (Basel, Switzerland).

Results

Validation of Ca-dye-based assay of recombinant Ca_v3 T-type Ca^{2+} channels

HEK293 cells are widely used to characterize voltage-gated channels because they have little or no endogenous channels under normal culture conditions, and because they express high levels of protein from plasmids containing the cytomegalovirus promoter. These cells have proven useful for studying T-channels as well,[21] and robust currents can be measured using either conventional or planar patch clamp recording (Fig. 1). To develop a Ca-dye-based assay, these cells were loaded with Fluo-4-AM, washed, and then assayed using a FlexStation. Addition of Ca^{2+} (10 m*M* final concentration) led to an increase in fluorescence in cells transfected with $Ca_v3.2$, but not in untransfected cells (Fig. 2A). This Ca-induced

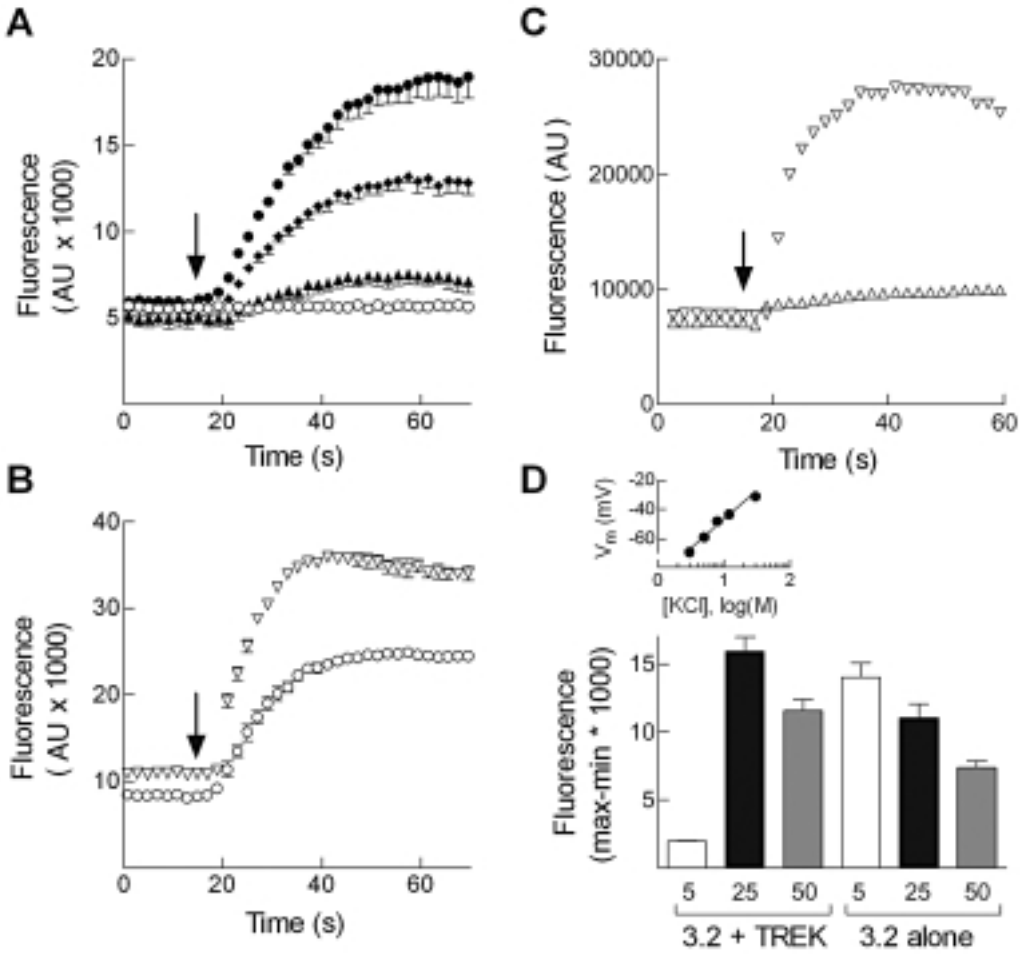

FIG. 2. Characterization of dye-based assay using a FlexStation. (**A**) HEK293 cells were loaded with Fluo-4, and then their fluorescent signal was monitored. Using the integrated fluidics, a bolus of $CaCl_2$ was delivered after reading 15 s of baseline, resulting in an increase in the Ca^{2+} concentration from 1.5 to 10 m*M*. In control nontransfected cells (○) there was no response to this addition. In stable cell lines selected for $Ca_v3.2$ expression, Ca^{2+} addition resulted in a rapid rise in fluorescent signal. This signal was blocked in cells that had been preincubated with 0.3 μM mibefradil (◆). Control (●), 10 μM mibefradil (▲). Data are the average of three replicates from a single plate. AU, arbitrary units. (**B**) A similar rise in fluorescence was detected in cell lines expressing either $Ca_v3.1$ (○) or $Ca_v3.3$ (▽). The arrow indicates addition of Ca. (**C**) In a cell line engineered to express both $Ca_v3.2$ and the K^+ leak channel TREK-1, the addition (arrow) of Ca^{2+} (△) induced next to no rise in fluorescence. Nevertheless, co-addition of KCl (final concentration 25 m*M*) along with $CaCl_2$ (▽) led to a large and rapid rise in fluorescence. In contrast, in the cell line expressing $Ca_v3.2$ alone, robust rises in fluorescence were observed after addition of either KCl alone or KCl + $CaCl_2$ (data not shown). (**D**) Effect of varying KCl on the Ca-induced fluorescent signal in $Ca_v3.2$ + TREK and $Ca_v3.2$ alone cells. (**Inset**) Measurement of membrane potential (V_m) as a function of KCl concentration. V_m was estimated using a ramp protocol as described previously.[19] Data represent average of three to 14 cells. The solid line represents a fit to the data with the Nernst equation. In cells expressing both $Ca_v3.2$ and TREK-1, Ca-induced fluorescence in the FlexStation assay showed a biphasic response with a peak at 25 m*M* KCl, which corresponds to a V_m of −31 mV. In contrast, in cells expressing $Ca_v3.2$ alone, increasing KCl only decreased the Ca-induced signal. Data are average and standard error of the mean from two experiments performed in triplicate.

signal in $Ca_v3.2$ cells could be attenuated by preincubation with mibefradil (Fig. 2A). A similar Ca-induced rise in fluorescence was measured in stable cell lines expressing human recombinant $Ca_v3.1$ and $Ca_v3.3$ (Fig. 2B). The Ca-dye signal was proportional to the size of the currents measured by whole cell electrophysiology, with the $Ca_v3.3$ line expressing the largest signal in both assays. If these signals were attributable to window currents via T-channels, which typically operate between -80 and -30 mV,[1] then hyperpolarization of the cell membrane would be expected to eliminate the current, and make it responsive to depolarization. This hypothesis was tested in a cell line expressing both $Ca_v3.2$ and a K^+ channel that is open at rest (leak channel), such as TREK-1.[22] The resting membrane potential of these cells is -83 mV.[19] Addition of Ca alone to these cells did not induce a fluorescent signal. Simultaneous addition of $CaCl_2$ and 25 m*M* KCl to these cells produced a robust fluorescent signal in the FlexStation assay (Fig. 2C). As predicted from the Nernst equation, the membrane potential could be adjusted by increasing the concentration of KCl in the $Ca_v3.2$-TREK cell line (Fig. 2D, inset). Accordingly, these cells exhibited a biphasic response to increasing concentrations of KCl (Fig. 2D), showing a small response to 5 m*M* KCl ($V_m = -60$ mV), peaking at 25 m*M* ($V_m = -31$ mV), and then falling at 50 m*M* ($V_m = -19$ mV). These responses are consistent with the voltage dependence of T-window currents.[1] In contrast, the cell line expressing $Ca_v3.2$ alone showed only a decrease in fluorescence as KCl was increased. Since the maximal responses in both cell lines were similar (Fig. 2D), we conclude that the membrane potential of the $Ca_v3.2$ alone cell line was already near optimal for the window current under control conditions. These results establish that $Ca_v3.2$ window currents underlie the increase in fluorescence detected after a bolus of Ca is added, and support the use of this signal in a high throughput assay. Although both cell lines produced similar signals under appropriate conditions, we selected the $Ca_v3.2$ alone cell line for further study because of the possibility that drugs might modulate TREK channel activity, thereby obscuring their effect on the T-channel.

Optimization of FlexStation and FLIPR assay conditions

Cell density. Cell densities used in fluorescence assays vary depending on the individual cell line and attachment to matrix-coated plates. We routinely used the 96-well microtiter plates coated with poly-D-lysine. We tested a range of the cell seeding density from 30,000 to 100,000 cells per well for 96-well plates and found the optimal cell density to be 60,000–80,000. After overnight culture (10–12 h) a uniform, 80–90% confluent monolayer was formed on the day of the assay. Cell plate signal tests indicated by the CV% varied from 8% to 12% among the three cell lines ("yellow" plate background signal tests were around 1.5–3% in the FLIPR). The CV of each cell plate has direct effects on the consistency and reproducibility of the measurements. After pipettor dispensing (adding a high Ca solution) and/or compounding (without the optional mixing function), we rechecked the cell signal test and found that CV had increased to 15–30%, with the largest increase in the $Ca_v3.3$ cells. In view of the disturbance of addition caused by FLIPR, we used manual compound addition 20 min prior to the FLIPR measurement.

Fluorescent dye indicators. The FLIPR Calcium 3 Assay Kit is a fluorescence calcium indicator reagent that provides a no-wash assay format. We initially compared this no-wash dye method with the conventional incubate and wash assay using Fluo-4-AM. There was no difference in the signal-to-noise ratio ($\sim$2.5) between these two dyes.

Trace metals such as zinc block $Ca_v3.2$ with at low micromolar concentrations.[23] Therefore we tested the effect of adding the chelator diethylenetriamine pentaacetic acid in the Fluo-4-AM loading step. We chose a diethylenetriamine pentaacetic acid concentration (1.2 m*M*) that would also reduce free Ca^{2+} (buffer made with 1.3 m*M* $CaCl_2$), but still maintain sufficient Ca^{2+} to keep cells adherent ($\sim$0.1 m*M*).

Determination of optimized $[Ca^{2+}]_o$ to induce the response

To establish the concentration–response of $[Ca^{2+}]_o$, we used four to eight wells per concentration. The replicates within the experiment yielded similar results, showing that a large signal can be induced by 10–20 m*M* $[Ca^{2+}]_o$ in the recombinant cells (Fig. 3A and B), but not in untransfected cells (data not shown). This Ca-induced signal was approximately half the size observed after addition of the Ca ionophore ionomycin (Fig. 3, column 6). Since high divalent cation concentrations can reduce the apparent potency of mibefradil,[24] we routinely used 10 m*M* $[Ca^{2+}]_o$ in all subsequent experiments unless specified otherwise.

Incubation durations and temperature. Most Ca-dye assays require probenecid, an anion exchange protein inhibitor, to block extrusion of the dye from the cell. Since both the fluorescent dyes and probenecid are toxic to cells, we conducted an experiment on the loading duration (20–60 min) and temperature (room temperature vs. 37°C). In both the FlexStation and FLIPR assay, there was no effect of changing the loading time in this range, and similar results were observed at either temperature (data not shown).

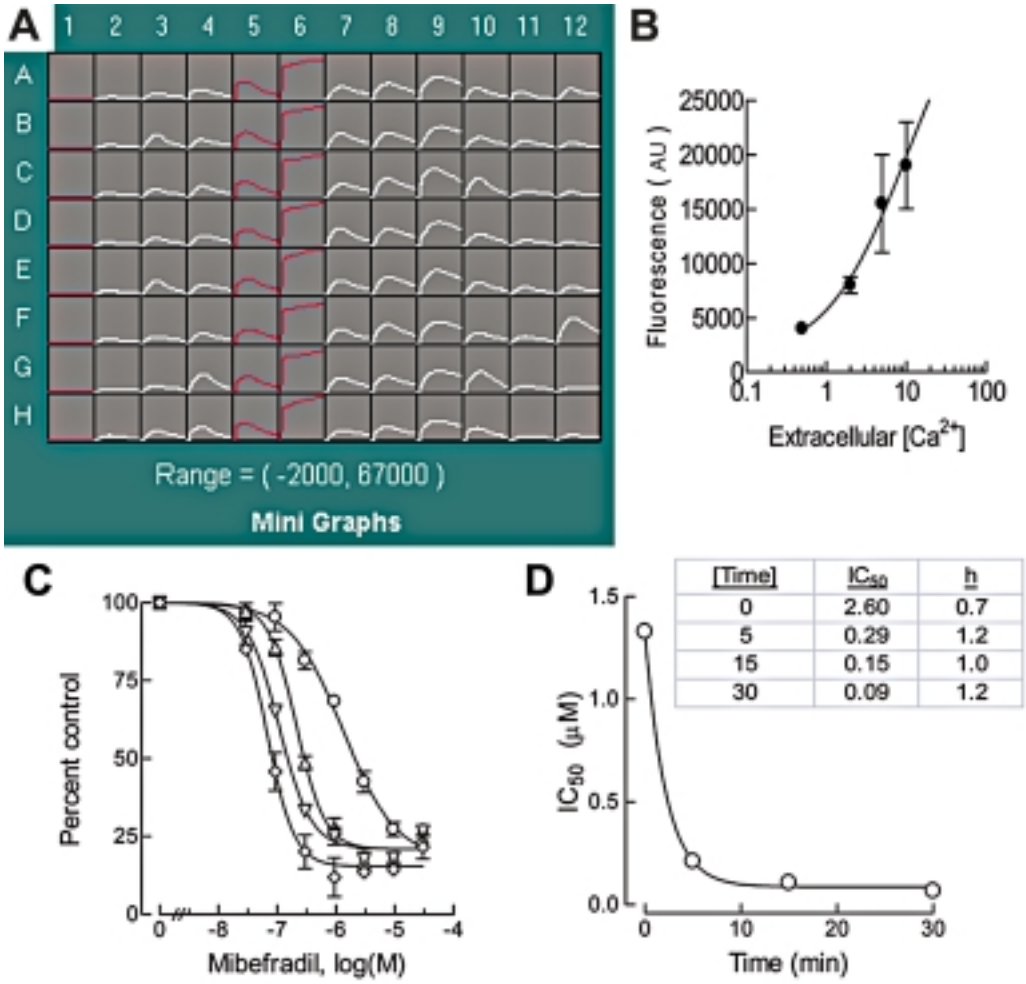

FIG. 3. Assay optimization. The effects of increasing $[Ca^{2+}]_o$ and ionomycin on $[Ca^{2+}]_i$ in $Ca_v3.2$-HEK293 cells were measured using FLIPR assay. (**A**) Raw traces of an entire 96-well plate. Columns 1 (adding 0.5 m*M* Ca^{2+} buffer), 5 (20 m*M* Ca^{2+}), and 6 (0.5 m*M* Ca^{2+} plus 3 μM ionomycin) are highlighted in red. Columns 7–12 were evoked by 10 m*M* Ca^{2+} and pretreated with different drugs (some showed inhibition). (**B**) Summary plot showing the increase in fluorescent dye signal as a function of increasing $CaCl_2$ concentration. Raw data are shown in (A), columns 2–5. AU, arbitrary units. (**C**) Mibefradil dose–response relationships obtained after incubation of $Ca_v3.2$ cells with mibefradil for varying times: (○), 0 min; (△), 5 min; (▽), 15 min; and (◇) 30 min. Data were obtained using the FlexStation assay. (**D**) The data shown in (C) were fit with the Hill-Langmuir equation, and the deduced IC_{50} was plotted as a function of incubation. (**Inset**) Values of IC_{50} and the Hill coefficient (*h*).

Binding rates of calcium channel blockers to L-type channels are time dependent, requiring at least 10 min to reach equilibrium.[25] To test time dependence, $Ca_v3.2$ cells were incubated with mibefradil for varying times at 37°C, and then the response to 10 m*M* Ca^{2+} was measured in the FlexStation assay. Simultaneous addition of Ca + mibefradil did produce block, but mibefradil potency was enhanced by preincubation, approaching a maximum at incubation times >15 min (Fig. 3C and D). Subsequent studies were performed after 30 min of incubation.

Drug block in the FLIPR assay. Each concentration was tested in four wells, and most compounds were tested twice. The IC_{50} values for those compounds that produced greater than 50% inhibition were automatically calculated using SRI software. Mibefradil produced a concentration-dependent inhibition of the Ca-dye signal in all three cell lines. A typical experiment testing mibefradil (columns 1–6) and lamotrigine (columns 7–12) is shown in Fig. 4A. Superimposed traces taken in the presence of varying concentrations are shown in Fig. 4B. Mibefradil displayed an IC_{50} of 1.8 μM when using $Ca_v3.1$-expressing cells (Fig. 4C, $n = 4$). In contrast, the Na^+ channel blocker lamotrigine produced only weak block ($IC_{50} = 550$ μM), suggesting that its antiseizure effects in childhood absence epilepsy is unlikely to be through the direct modulation of the T-type current. Typ-

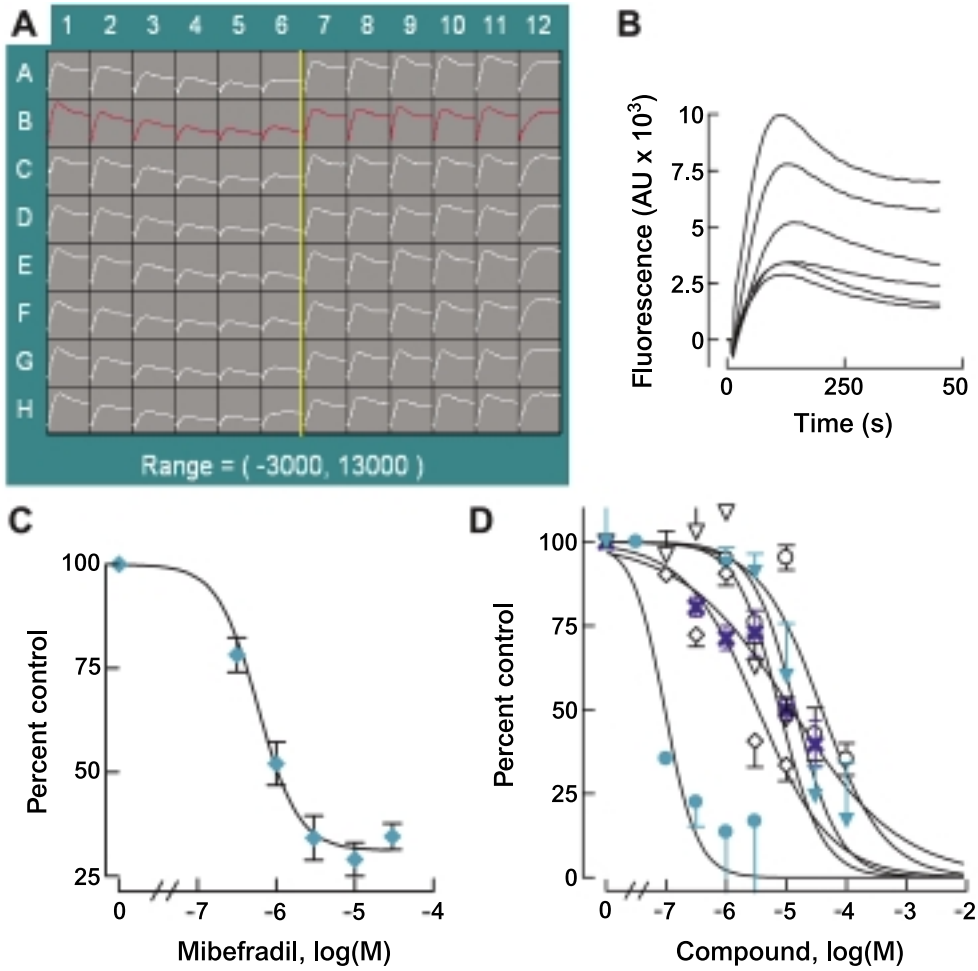

FIG. 4. Drug-induced block of $Ca_v3.1$ channels as measured by FLIPR assay. Cells were pretreated with increasing concentrations of either mibefradil (columns 1–6) or lamotrigine (columns 7–12). (**A**) Raw traces of fluorescent signal recorded across an entire 96-well plate seeded with $Ca_v3.1$. Compounds were preincubated in the plates for 20 min prior to FLIPR measurements. The Ca^{2+} signal was triggered by the FLIPR addition of $CaCl_2$, thereby raising extracellular Ca^{2+} to 10 m*M*. Measurements of each concentration were made in one column (eight wells). Columns 1–6 are 0, 0.3, 1, 3, 10, and 30 μM mibefradil, respectively; columns 7–12 are 0, 3, 10, 30, 100, and 300 μM lamotrigine, respectively. (**B**) Representative traces obtained in control cells and in the presence of mibefradil [(highlighted in red in (A)] are superimposed. AU, arbitrary units. (**C**) Average mibefradil dose–response obtained in the FLIPR assay of $Ca_v3.1$ cells ($n = 4$). Maximal block averaged 70%, and taking this into account yields an IC_{50} of 0.6 μM (smooth curve). (**D**) Dose–response curves of a set of compounds: fendiline (▼), fluphenazine (▽), nifedipine (○), penfluridol (◇), perhexiline (×), and pimozide (●). Each concentration was tested in quadruplicate. For display purposes, the smooth curves are fits to the data where maximal block was fixed at 100%.

ical dose–responses to six compounds are shown in Fig. 4D.

The Ca-induced signal often oscillated in $Ca_v3.3$ cells compared to the other two subtypes (Fig. 5). In the FLEX assay, low (0.1 μM) concentrations of mibefradil slowed the response to Ca with little or no effect on the maximum fluorescence observed, while higher concentrations blocked the signal almost completely. These oscillations were more apparent in the FLIPR assay because of the higher sampling frequency (Fig. 5B).

Comparison of drug block among the FLIPR assay, IonWorks HTS assay, and conventional patch clamp recording. To evaluate the fluorometric assay for HTS, we further conducted a comparative pharmacologic study on a set of known ion channel blockers. A variety of structurally diverse compounds, including phenylalkylamines (*e.g.*, mibefradil), dihydropyridines (*e.g.*, nifedipine), and piperidine antipsychotics (*e.g.*, pimozide) were tested by both the FLIPR assay and patch clamp recordings. For compounds with known potency, their IC_{50} values were used as a guideline,[26] while compounds with unknown potency were typically tested at 1, 3, 10, 30, and 100 μM (maximal DMSO of 0.1%). The same sets of compounds were tested using an IonWorks HT patch system. Initial patch recordings under current clamp

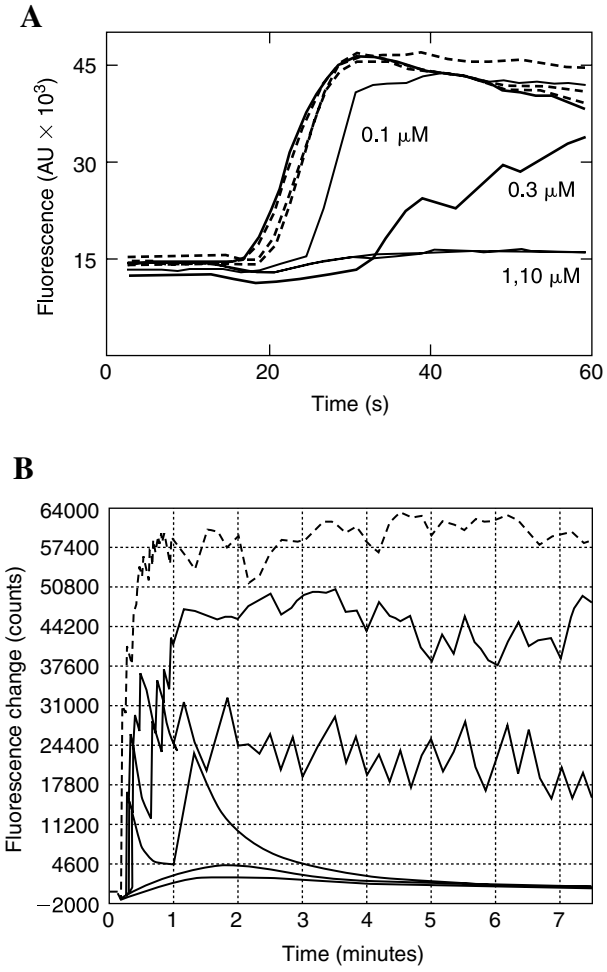

FIG. 5. $Ca_v3.3$ cell line shows oscillations in intracellular calcium. (**A**) FlexStation data obtained using the cell line LT9-5 expressing the human recombinant $Ca_v3.3a$ splice variant. Cells were pretreated for 30 min at 37°C with varying doses of mibefradil (as indicated). After 15 s of baseline recording, a bolus of $CaCl_2$ was added to increase its concentration to 10 m*M*. Control is shown with a thick line. Responses are from a single well, but are typical of the other two replicates run on the same plate. Not all experiments showed the oscillations, but in all cases drug block began with a slowing of the time to peak. AU, arbitrary units. (**B**) Responses measured using a FLIPR from the same $Ca_v3.3a$ cell line. Experimental conditions were similar to the FlexStation assay except the preincubation was for 20 min at room temperature.

mode revealed resting potentials of Ca_v3 cells that varied between −15 to −40 mV. Compounds were tested in voltage clamp mode using a protocol consisting of a depolarizing test pulse to −30 mV for 500 ms, then a return to a holding potential (V_h) of −100 mV for 5 s, followed by a voltage ramp from −100 to +20 mV over 800 ms. Although the whole-cell seal resistances were between 150 and 300 MΩ, the signal-to-noise ratio is excellent. T-current amplitudes ranged from 50 to 500 pA under our experimental conditions (Figs. 1B and 6A). Optimization of cell culture, cell preparation conditions, and recording solutions improved seal resistance, stability, and overall success, increasing the patching rate from 30% to 60%. Baseline current traces (precompound) were almost superimposable with those recorded 10 s after 0.5% DMSO was applied as a control, indicating the stability of the currents recorded. Applications of several compounds (3.5 μl per well) produced inhibition of the T-current in a concentration-dependent manner (Fig. 6B). Each 384-well planar patch assay took about 1 h under this specific protocol, and one technician could conduct recordings on six to eight plates per day. A subset of compounds were also tested in conventional patch clamp recording using similar assay conditions (representative traces shown in Fig. 6C, inset). Linear regression analysis of the IC_{50} values obtained in the two assays yielded a line with a slope of 0.6 ± 0.2 and a correlation coefficient of 0.8 (Fig. 6C). Therefore the IonWorks produces reliable estimates of drug potency, although these estimates were approximately twofold lower than observed with the "gold standard" conventional patch clamp recording. Linear regression analysis of the IC_{50} values obtained with FLIPR to manual patch clamp showed a steeper slope (0.7), but more scatter (Fig. 6D). Comparison of the IonWorks results to those obtained with FLIPR again showed a slope that differed significantly from 1 (0.54), and a high correlation (Fig. 6E). A similar discrepancy was reported previously, and a likely mechanism was proposed: drugs have higher affinities for inactivated states that predominate in the FLIPR assay compared to the rested states achieved in cells voltage clamped to −90 mV.[18] Accordingly, comparison of results obtained with eight compounds using the FlexStation and FLIPR assays showed a higher slope (0.7; data not shown).

Discussion

The main goal of this study was to establish the mechanism by which recombinant T-channels are capable of regulating intracellular calcium, and validate the use of this property for HTS. Our initial hypothesis was that T-channels were capable of opening at the resting membrane potential of HEK293 cells. This property has been extensively studied in thalamic neurons, and contributes to their bistability: the ability to be have two distinct "resting" membrane potentials.[16] Recombinant T-channels also show the ability to generate persistent window currents, which has been estimated at ~2% of the total whole cell T-current.[27,28] It was suggested that this window current was sufficient to increase intracellular Ca^{2+} in HEK293 cells as detected by Ca-sensitive fluorescent dyes,[17] and that this signal could be used for a FLIPR assay.[18] We show that co-expression of $Ca_v3.2$ with a K^+

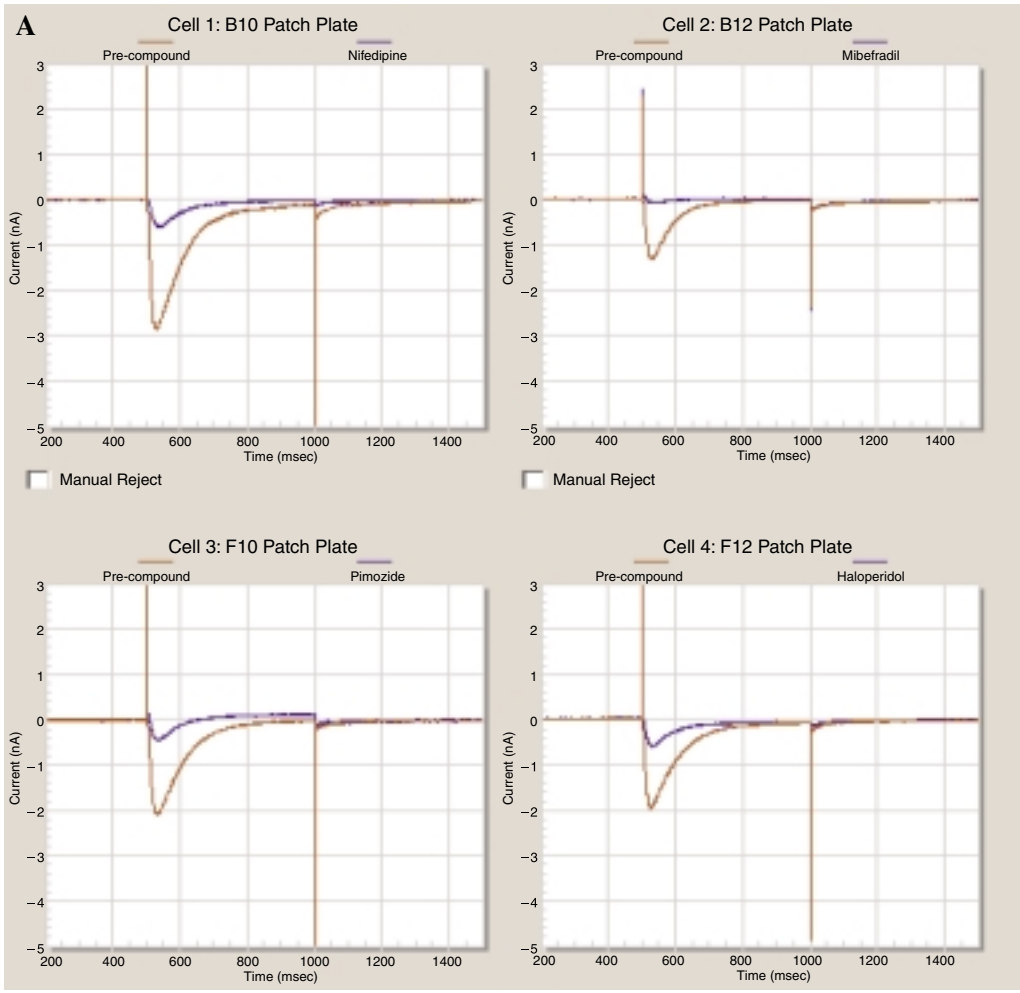
A
Cell 1: B10 Patch Plate
Pre-compound
Nifedipine
Cell 2: B12 Patch Plate
Pre-compound
Mibefradil
Cell 3: F10 Patch Plate
Pre-compound
Pimozide
Cell 4: F12 Patch Plate
Pre-compound
Haloperidol
Current (nA)
Time (msec)
Manual Reject

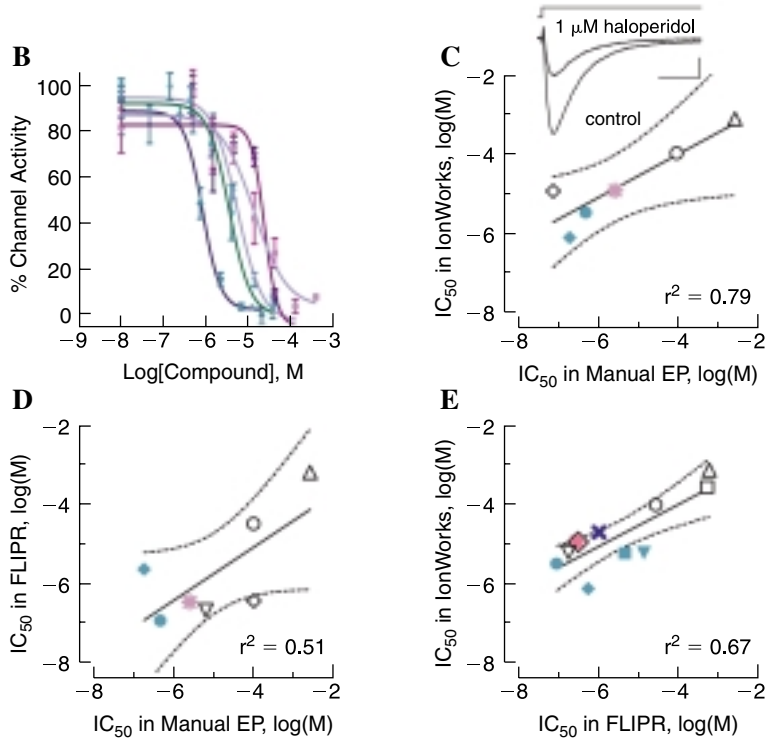
B
% Channel Activity
Log[Compound], M
C
1 μM haloperidol
control
IC50 in IonWorks, log(M)
IC50 in Manual EP, log(M)
r2 = 0.79
D
IC50 in FLIPR, log(M)
IC50 in Manual EP, log(M)
r2 = 0.51
E
IC50 in IonWorks, log(M)
IC50 in FLIPR, log(M)
r2 = 0.67

FIG. 6.

channel that is capable of hyperpolarizing the plasma membrane potential[29] eliminates this signal. The resting membrane potential of these cells is approximately −80 mV, and can be depolarized by increasing external K^+.[19] Consistent with this property, we show that the Ca-dye signal can be restored in this cell line by co-addition of Ca^{2+} plus K^+. These results establish that the window current underlies the Ca-dye response observed when the Ca is elevated above 2 m*M*. We show that this response can be reliably measured in stably transfected cell lines that express one of the three recombinant Ca_v3 channels at high levels using either a FlexStation or FLIPR. Another goal of this study was to optimize the FLIPR assay for primary HTS. We also show that these cell lines are useful for secondary screening using IonWorks, an automated planar patch clamp system. Finally we validate the FLIPR assay by comparing the potency of known Ca^{2+} channel blockers to that obtained using patch clamp electrophysiology. Similar estimates of potency have been obtained for haloperidol, mibefradil, nifedipine, pimozide, and penfluridol using manual patch clamp electrophysiology on native T-currents.[26] Therefore these methods and cell lines should be useful for HTS of compound libraries.

A selective T-channel antagonist may be useful in a variety of diseases. Recent genetic analysis of the gene encoding $Ca_v3.2$, *CACNA1H*, uncovered the presence of mutations that were only found in patients with childhood absence epilepsy.[30] Subsequent studies have shown that these mutations alter channel behavior and their trafficking to the cell surface.[28,31] Antiepileptic drugs such as ethosuximide are useful for the treatment of absence epilepsy. Ethosuximide (at concentrations >0.1 m*M*) is capable of blocking native and recombinant T-channels, providing further support for the notion that a novel, more potent, and selective T-channel blocker would be a useful antiepileptic.[21,32] Such a drug may also be useful in temporal lobe epilepsy based on the observation that T-currents are up-regulated in the pilocarpine model: more than 50% of rat CA1 pyramidal cells, which normally fire in regular single action potentials, are persistently converted to a bursting mode in pilocarpine-treated animals.[33] This change resulted from up-regulation of T-type currents and underlies a long-lasting modification of neuronal firing. Other antiepileptic drugs that have been shown to block T-currents are lamotrigine and zonisamide; however, like ethosuximide, they are weak and nonspecific.[34–36]

T-channel blockers may also be useful antihypertensives. The ability of mibefradil to normalize high blood pressure and to block T-type channels generated much interest in the physiology and pharmacology of the T-type channels in the cardiovascular system.[37] However, mibefradil had to be withdrawn from the market because of drug–drug interactions. The ability of certain dihydropyridines such as efonidipine to block both T- and L-type channels may confer additional clinical benefit over selective L-type blockers in terms of reducing both glomerular nephritis and plasma aldosterone levels.[38,39]

Recent studies have suggested some new indications for T-channel blockers, including analgesia and neuroprotection.[4,40,41] Inhibition of T-type currents may be useful in the treatment of neuropathic pain, based on experimental evidence obtained using mibefradil[42] or ethosuximide in animals.[43,44] The novel neuroprotective compounds 619C89 and SB-209712 potently block T-currents at submicromolar concentrations, and this inhibition is thought to contribute to the neuroprotective effects of these compounds. However, these drugs also potently block voltage-gated Na^+ channels, high-voltage-activated Ca^{2+} channels, and the delayed rectifying outward K^+ current. This poor selectivity in ion channel modulation may be associated with their side effects.[45,46] In conclusion, a selective T-channel blocker may be useful in a variety of diseases, and HTS of recombinant channels may provide a useful assay for drug discovery.

Acknowledgments

We thank Michael Johnson and Kevin Lynch for help with the FlexStation assay. We thank Robert Petroski and Joseph McGivern for helpful discussions. This work was supported by grants NS050771 (to X.X.), HL36977 (to P.Q.B.), and NS38691 (to E.P.-R.) from the National Institutes of Health.

FIG. 6. Planar patch clamp recording of $Ca_v3.1$ currents. (**A**) Sample current traces recorded during a holding potential of −100 mV and depolarizing pulse to −30 mV for 500 ms. Each panel shows the response measured before (control) and after application of an individual drug (10 μM) indicated. (**B**) Dose–response of five reference compounds determined using the IonWorks Quattro system (n = 3–8 cells per concentration): fendiline (▼), mibefradil (◆), perhexiline (×), haloperidol (*), and pimozide (●). (**C**) Correlation plot with linear regression analysis (Prism) of the IC_{50} values obtained using IonWorks to that obtained with conventional patch clamp electrophysiology (EP): fluphenazine (▽), penfluridol (◇), nifedipine (○), lamotrigine (□), ethosuximide (△), and promethazine (■) plus compounds in (B). (**Inset**) Representative current traces obtained by manual patch clamp before (control) and during exposure to 1 μM haloperidol. Scale bar = 100 pA and 25 ms. The correlation line is shown with the 95% confidence limits (dotted lines). The ethosuximide result was published previously.[21] (**D** and **E**) Correlation of the data obtained in FLIPR assay to that obtained in either (D) manual patch clamp electrophysiology or (E) with IonWorks.

References

1. Perez-Reyes E: Molecular physiology of low-voltage-activated T-type calcium channels. *Physiol Rev* 2003;83: 117–161.
2. Llinás RR, Ribary U, Jeanmonod D, Kronberg E, Mitra PP: Thalamocortical dysrhythmia: a neurological and neuropsychiatric syndrome characterized by magnetoencephalography. *Proc Natl Acad Sci U S A* 1999;96: 15222–15227.
3. Nelson MT, Joksovic PM, Perez-Reyes E, Todorovic SM: The endogenous redox agent L-cysteine induces T-type Ca^{2+} channel-dependent sensitization of a novel subpopulation of rat peripheral nociceptors. *J Neurosci* 2005;25: 8766–8775.
4. Nelson M, Todorovic S, Perez-Reyes E: The role of T-type calcium channels in epilepsy and pain. *Curr Pharm Des* 2006;12:2189–2197.
5. Moosmang S, Haider N, Bruderl B, Welling A, Hofmann F: Antihypertensive effects of the putative T-type calcium channel antagonist mibefradil are mediated by the L-type calcium channel $Ca_v1.2$. *Circ Res* 2006;98:105–110.
6. Kim D, Song I, Keum S, Lee T, Jeong MJ, Kim SS, *et al.*: Lack of the burst firing of thalamocortical relay neurons and resistance to absence seizures in mice lacking α1G T-type Ca^{2+} channels. *Neuron* 2001;31:35–45.
7. Anderson MP, Mochizuki T, Xie J, Fischler W, Manger JP, Talley EM, *et al.*: Thalamic $Ca_v3.1$ T-type Ca^{2+} channel plays a crucial role in stabilizing sleep. *Proc Natl Acad Sci U S A* 2005;102:1743–1748.
8. Todorovic SM, Jevtovic-Todorovic V, Meyenburg A, Mennerick S, Perez-Reyes E, Romano C, *et al.*: Redox modulation of T-type calcium channels in rat peripheral nociceptors. *Neuron* 2001;31:75–85.
9. Dogrul A, Gardell L, Ossipov M, Tulunay F, Lai J, Porreca F: Reversal of experimental neuropathic pain by T-type calcium channel blockers. *Pain* 2003;105:159–168.
10. Gibbs JW 3rd, Zhang YF, Ahmed HS, Coulter DA: Anticonvulsant actions of lamotrigine on spontaneous thalamocortical rhythms. *Epilepsia* 2002;43:342–349.
11. Bourinet E, Alloui A, Monteil A, Barrere C, Couette B, Poirot O, *et al.*: Silencing of the Cav3.2 T-type calcium channel gene in sensory neurons demonstrates its major role in nociception. *EMBO J* 2005;24:315–324.
12. Choi S, Na HS, Kim J, Lee J, Lee S, Kim D, *et al.*: Attenuated pain responses in mice lacking Ca3.2 T-type channels. *Genes Brain Behav* 2006 Aug 29; [Epub ahead of print].
13. Gomora JC, Murbartián J, Arias JM, Lee J-H, Perez-Reyes E: Cloning and expression of the human T-type channel $Ca_v3.3$: insights into prepulse facilitation. *Biophys J* 2002; 83:229–241.
14. Schroeder K, Neagle B, Trezise DJ, Worley J: Ionworks HT: a new high-throughput electrophysiology measurement platform. *J Biomol Screen* 2003;8:50–64.
15. Trumbull JD, Maslana ES, McKenna DG, Nemcek TA, Niforatos W, Pan JY, *et al.*: High throughput electrophysiology using a fully automated, multiplexed recording system. *Recept Channels* 2003;9:19–28.
16. Crunelli V, Toth TI, Cope DW, Blethyn K, Hughes SW: The 'window' T-type calcium current in brain dynamics of different behavioural states. *J Physiol (Lond)* 2005;562: 121–129.
17. Chemin J, Monteil A, Briquaire C, Richard S, Perez-Reyes E, Nargeot J, *et al.*: Overexpression of T-type calcium channels in HEK-293 cells increases intracellular calcium without affecting cellular proliferation. *FEBS Lett* 2000; 478:166–172.
18. Xia M, Imredy J, Santarelli V, Liang H, Condra C, Bennett P, *et al.*: Generation and characterization of a cell line with inducible expression of $Ca_v3.2$ (T-type) channels. *Assay Drug Dev Technol* 2003;1:637–645.
19. Yao J, Davies LA, Howard JD, Adney SK, Welsby PJ, Howell N, *et al.*: Molecular basis for the modulation of native T-type Ca^{2+} channels in vivo by Ca^{2+}/calmodulin-dependent protein kinase II. *J Clin Invest* 2006;116: 2403–2412.
20. Zhang JH, Chung TD, Oldenburg KR: A simple statistical parameter for use in evaluation and validation of high throughput screening assays. *J Biomol Screen* 1999;4: 67–73.
21. Gomora JC, Daud AN, Weiergräber M, Perez-Reyes E: Block of cloned human T-type calcium channels by succinimide antiepileptic drugs. *Mol Pharmacol* 2001;60: 1121–1132.
22. Maingret F, Lauritzen I, Patel AJ, Heurteaux C, Reyes R, Lesage F, *et al.*: TREK-1 is a heat-activated background K^+ channel. *EMBO J* 2000;19:2483–2491.
23. Traboulsie A, Chemin J, Chevalier M, Quignard JF, Nargeot J, Lory P: Subunit-specific modulation of T-type calcium channels by zinc. *J Physiol* 2007;578(Pt 1):159–171.
24. Martin RL, Lee JH, Cribbs LL, Perez-Reyes E, Hanck DA: Mibefradil block of cloned T-type calcium channels. *J Pharmacol Exp Ther* 2000;295:302–308.
25. Fosset M, Jaimovich E, Delpont E, Lazdunski M: [^{3}H]Nitrendipine receptors in skeletal muscle. *J Biol Chem* 1983; 258:6086–6092.
26. Heady TN, Gomora JC, Macdonald TL, Perez-Reyes E: Molecular pharmacology of T-type Ca^{2+} channels. *Jpn J Pharmacol* 2001;85:339–350.
27. Serrano JR, Perez-Reyes E, Jones SW: State-dependent inactivation of the α1G T-type calcium channel. *J Gen Physiol* 1999;114:185–201.
28. Vitko I, Chen Y, Arias JM, Shen Y, Wu XR, Perez-Reyes E: Functional characterization and neuronal modeling of the effects of childhood absence epilepsy variants of *CACNA1H*, a T-type calcium channel. *J Neurosci* 2005;25: 4844–4855.
29. Talley EM, Lei Q, Sirois JE, Bayliss D A: TASK-1, a two-pore domain K^+ channel, is modulated by multiple neurotransmitters in motoneurons. *Neuron* 2000;25:399–410.
30. Chen YC, Lu JJ, Pan H, Zhang YH, Wu HS, Xu KM, *et al.*: Association between genetic variation of CACNA1H and childhood absence epilepsy. *Ann Neurol* 2003;54: 239–243.
31. Vitko I, Bidaud I, Arias JM, Mezghrani A, Lory P, Perez-Reyes E: The I–II loop controls plasma membrane expression and gating of $Ca_v3.2$ T-type Ca^{2+} channels: a paradigm for CAE mutations. *J Neurosci* 2007;27:322–330.
32. Coulter DA, Huguenard JR, Prince DA: Characterization of ethosuximide reduction of low-threshold calcium current in thalamic neurons. *Ann Neurol* 1989;25:582–593.
33. Su H, Sochivko D, Becker A, Chen J, Jiang Y, Yaari Y, *et al.*: Upregulation of a T-type Ca^{2+} channel causes a long-lasting modification of neuronal firing mode after status epilepticus. *J Neurosci* 2002;22:3645–3655.
34. Leresche N, Parri HR, Erdemli G, Guyon A, Turner JP, Williams SR, *et al.*: On the action of the anti-absence drug ethosuximide in the rat and cat thalamus. *J Neurosci* 1998; 18:4842–4853.
35. Xie X, Lancaster B, Peakman T, Garthwaite J: Interaction of the antiepileptic drug lamotrigine with recombinant rat

brain type IIA Na^+ channels and with native Na^+ channels in rat hippocampal neurones. *Pflugers Arch* 1995;430: 437–446.
36. Sobieszek G, Borowicz KK, Kimber-Trojnar Z, Malek R, Piskorska B, Czuczwar SJ: Zonisamide: a new antiepileptic drug. *Pol J Pharmacol* 2003;55:683–689.
37. Tsien RW, Clozel JP, Nargeot, J, eds.: *Low Voltage-Activated T-Type Calcium Channels*. Adis International Ltd., Chester, UK, 1998.
38. Hayashi K, Ozawa Y, Fujiwara K, Wakino S, Kumagai H, Saruta T: Role of actions of calcium antagonists on efferent arterioles—with special references to glomerular hypertension. *Am J Nephrol* 2003;23:229–244.
39. Okayama S, Imagawa K, Naya N, Iwama H, Somekawa S, Kawata H, *et al.*: Blocking T-type Ca^{2+} channels with efonidipine decreased plasma aldosterone concentration in healthy volunteers. *Hypertens Res* 2006;29:493–497.
40. McGivern JG: Targeting N-type and T-type calcium channels for the treatment of pain. *Drug Discov Today* 2006;11:245–253.
41. Nikonenko I, Bancila M, Bloc A, Muller D, Bijlenga P: Inhibition of T-type calcium channels protects neurons from delayed ischemia-induced damage. *Mol Pharmacol* 2005; 68:84–89.
42. Todorovic SM, Meyenburg A, Jevtovic-Todorovic V: Mechanical and thermal antinociception in rats following systemic administration of mibefradil, a T-type calcium channel blocker. *Brain Res* 2002;951:336–340.
43. Flatters SJ, Bennett GJ: Ethosuximide reverses paclitaxel- and vincristine-induced painful peripheral neuropathy. *Pain* 2004;109:150–161.
44. Barton ME, Eberle EL, Shannon HE: The antihyperalgesic effects of the T-type calcium channel blockers ethosuximide, trimethadione, and mibefradil. *Eur J Pharmacol* 2005;521:79–85.
45. Xie XM, Garthwaite J: State-dependent inhibition of Na^+ currents by the neuroprotective agent 619C89 in rat hippocampal neurons and in a mammalian cell line expressing rat brain type IIA Na^+ channels. *Neuroscience* 1996;73951–962.
46. McNaughton NC, Hainsworth AH, Green PJ, Randall AD: Inhibition of recombinant low-voltage-activated Ca^{2+} channels by the neuroprotective agent BW619C89 (Sipatrigine). *Neuropharmacology* 2000;39:1247–1253.

Address reprint requests to:
Xinmin Simon Xie, Ph.D.
Bioscience Division
SRI International
333 Ravenswood Avenue
Menlo Park, CA 94250

E-mail: simon.xie@sri.com

or

Edward Perez-Reyes, Ph.D.
Department of Pharmacology and
Molecular Medicine Graduate Program
University of Virginia
P.O. Box 800735
Charlottesville, VA 22908

E-mail: eperez@virginia.edu